PERGAMON

Journal of Atmospheric and Solar-Terrestrial Physics 63 (2001) 915–924

Journal of ATMOSPHERIC AND SOLAR-TERRESTRIAL PHYSICS

www.elsevier.nl/locate/jastp

Disturbances of the western European ionosphere during the total solar eclipse of 11 August 1999 measured by a wide ionosonde and radar network

T. Farges[a], J.C. Jodogne[b], R. Bamford[c], Y. Le Roux[d], F. Gauthier[d], P.M. Vila[e,*], D. Altadill[f], J.G. Sole[f], G. Miro[g]

[a] *CEA/LDG, BP 12, 91860 Bruyères-le-Châtel, France*
[b] *Geophysics Division I.R.M. 3, Ave Circulaire, 1180 Brussels, Belgique*
[c] *RAL, Chilton, Didcot Oxon, UK*
[d] *CNE/DMR/TSI, France Telecom, 2 Ave P. Marzin, 22301 Lannion Cedex, France*
[e] *CETP/CNRS, 4 Ave Neptune, 94 107 St Maur-des-Fossés Cedex, France*
[f] *Observatori d'Ebre, 43520, Roquetes, TARRAGONA, Spain*
[g] *El ARENOSILLO Space Science Division, Mazagon-Moguer, 2110 HUELVA, Spain*

Received 12 October 1999; received in revised form 14 April 2000; accepted 12 June 2000

Abstract

The 11 August 1999 Solar eclipse totality path ran across western Europe at near-constant latitudes of about 49°N. It occurred at mid-time of a sequence of three days with steady solar wind and quiet magnetospheric conditions. Its response was observed by a score of ionospheric facilities, which will provide high-resolution probing of the various disturbances. First results allow us to compare the time fluctuations at various distances from totality on the eclipse and adjacent days, inside a 5° West to 5° East longitude area. In this preliminary work the foF1 and foF2 time changes are presented in contour maps on a 50 km size grid. They show the expected longitude transit of eclipse perturbation. We venture brief comments on the eclipse-own signatures as separate from the various wave oscillations detected prior to eclipse time by 12.4 MHz panoramic azimuth scans of the Losquet radar near Lannion (Brittanny).

Keywords: Ionospheric disturbances; Solar eclipse

1. Introduction

Solar eclipses are studied by ionospherists from the beginning of the ionosphere studies (Ratcliffe, 1956). Their disturbances provide a unique opportunity to understand the ionosphere formation and dynamic processes. The loss rate of the F region have been well analyzed by several authors (Rishbeth, 1968). Since 1970, a new interest has risen in solar eclipse studies, about the propagation of a gravity wave generated by the atmospheric cooling in the Moon shadow (Chimonas and Hines, 1970). When a solar eclipse affects a quiet-period ionosphere, we have a chance of drawing crucial tests about the characteristic response of the ionospheric plasmas to the set of perturbations imposed by the strong and well-defined occultation of the EUV and IR solar radiation.

However, recurrent ionospheric solar eclipse studies have brought many inconclusive results. No two solar eclipses produce the same plasma motion disturbances because, the lunar cone travel geometry and its angular effects on our magnetized plasmas are different each time (in fact our results suggest a longitude diversity of the disturbance between its pre-noon and post-noon phases). The present event benefited from the dense West European ionospheric network, and is a challenge to atmosphere and ionosphere models

* Corresponding author. Tel.: +33-1-45-11-4237.
E-mail addresses: farges@ldg.bruyeres.cea.fr (T. Farges), paul.vila@cetp.ipsl.fr (P.M. Vila).

1364-6826/01/$ - see front matter
PII: S1364-6826(00)00195-4

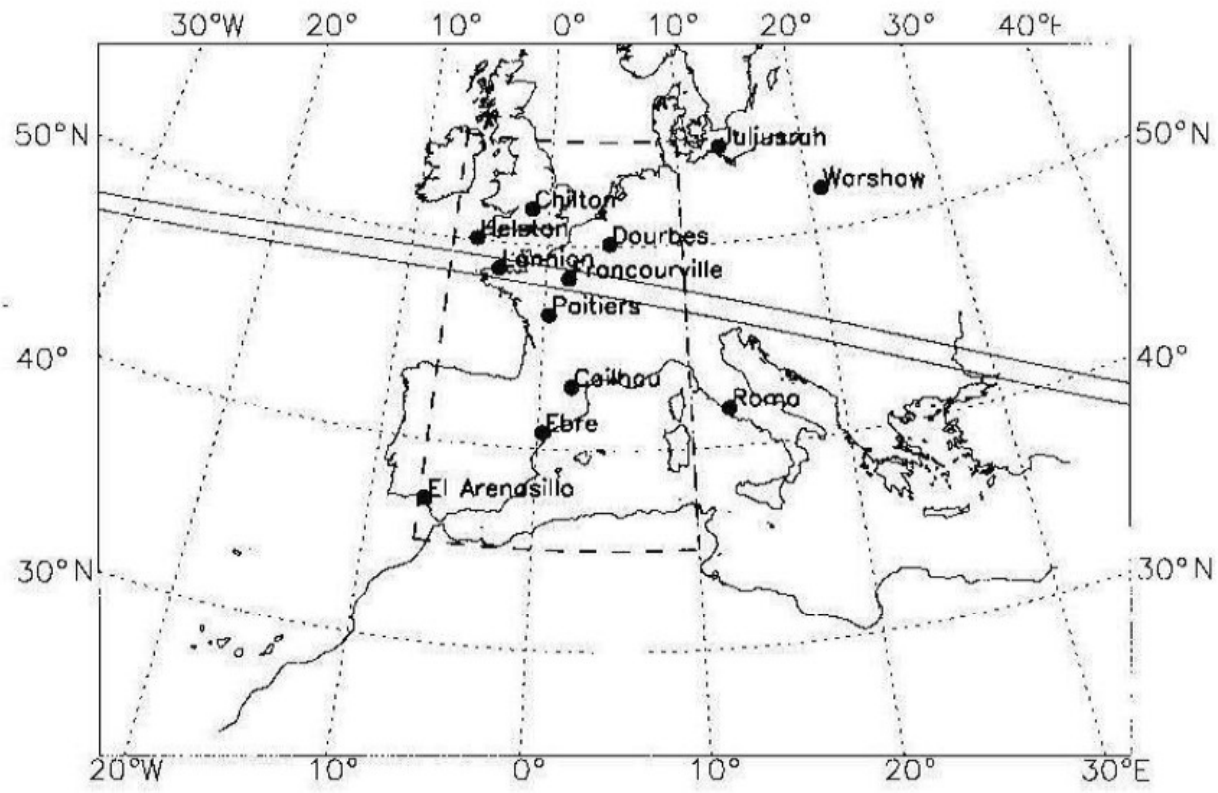

Fig. 1. Map of the total solar eclipse path at 200 km height on August 11, 1999, above Western Europe. Location of vertical incidence ionosondes used in the paper is indicated with circles.

e.g. TGCM (Ridley et al., 1984; Roble et al., 1986), CTIP (Müller-Wodarg et al., 1998)).

The improvements in cooperation and communication among European observers greatly facilitated the compilation of data. This allowed direct comparison of rapid variations in virtual height ionospheric profiles and in the various true height-frequency variations. Fig. 1 is a general map of the eclipsed earth domain with the frame encompassing our present West European area of study, expanded in Fig. 4. The magnetic activity indices were notably weak on the 10, 11 and 12 August 1999 with Kp values of 9, 12+ and 15+, respectively. The solar flux F10.7 was of 128. This makes it easier to visualize the main processes that disturbed the plasma on the eclipse day.

We here present a first look assessment of the simultaneous measurements from 12 vertical incidence (VI) ionosondes and some auxiliary radars. This rapid communication paper deals therefore with: a description of the experimental device and a qualitative description of the most salient eclipse characteristics, as well as gravity wave and other oscillations observed during the eclipse and on August 12, selected as controlled day in Section 2; Some quarter-hourly 2D maps of the foF1 and foF2 eclipse evolution over the geographic area: 5° West to 5° East by 35° to 55° North in Section 3; comments on the various perturbations visible on the present raw data, and on gravity wave typology, comparing the analogy variations in 2D-time across the West European network in Section 4.

2. Measurements in Western Europe during the solar eclipse

2.1. Experimental device

The observation of this solar eclipse benefited from an exceptional experimental cover in Western Europe. We present in Table 1, the characteristics of the 12 ionosondes used, with location, time resolution and maximum solar obscuration at 200 km height.

The HF sounding network of the Laboratoire de Detection et de Geophysique consists of a transmitter located in Francourville (FRC) and of three receivers which have been set in a radius of 60 km of FRC. The experiment is based on the propagation of an HF wave between a transmitter and a receiver through the ionosphere. This HF wave is reflected when its frequency is equal to the plasma frequency along the propagation path. Two sounding methods are used in parallel. The first method is vertical incidence ionograms which gives the electron density profile above FRC. The second method measures phase shifts due to ionospheric motions as gravity waves, or travelling ionospheric disturbances (TID). Phase shifts are measured by radar frequency Doppler spectra, which determine the vertical speed at the reflection point. If an itinerant perturbation affects the three links successively, the horizontal component of the perturbation velocity is determined by triangulation.

Table 1
Location of the ionosondes used during the eclipse measurements with their time resolution and their maximum solar obscuration at 200 km height

Station	Longitude	Latitude	Time resolution (min)	Maximum solar obscuration at 200 km height (%)
Francourville	1.7°E	48.4°N	1	100.0
Lannion	3.45°W	48.7°N	1	100.0
Helston	5.3°W	50.1°N	5	98.7
Dourbes	4.6°E	50.1°N	10	96.2
Chilton	1.3°W	51.7°N	4	92.3
Poitiers	0.3°E	46.6°N	15	92.1
Roma	12.5°W	41.9°N	5	83.3
Cailhau	2.1°E	43.1°N	0.5	81.2
Warshaw	21°W	52°N	5	79.1
Juliusruh	13.4°E	54.6°N	10	75.9
Ebre	0.3°E	40.8°N	5	71.6
El Arenosillo	6.7°W	37.1°N	15	55.7

Ionogram results are presented in this paper while the Doppler data will be thoroughly studied in a future paper.

The Losquet oblique bakscatter radar sounded volumes of the ionosphere at group-path distances of 300–1200 km from the radar, completing the VI ionosonde network.

2.2. *Losquet radar results*

The Losquet radar facility, near Lannion, has a circular array of 120 antennae scanned every 1.5 min. During the eclipse experiment, the frequency used was 12.4 MHz with an elevation angle around 30°. Any depletion in the F layer causes deeper penetration of the sounding wave, thus longer group path.

The oblique soundings presented in Fig. 2 correspond to F region reflecting areas from three azimuths (each panel showing two azimuth plots), respectively, located around the Northern Irish Sea (00–03°), the Southern Scotland East coast (24–27°), South-East of France (138–141°, Haute Provence) and North-West of Spain (198–201°). The range scale is given in return backscatter group path; hence the target is located at half this range.

Both northward sequences show eclipse-centered holes of width rapidly changing with azimuth, while the South-Eastward record clearly evidences a penetration disturbance of opposite symmetry to that of the northward sightings. For all azimuths the furthest group path time coincides exactly with the maximum obscuration time in the target reflection area concerned. The South-East to South-West-oriented series reveals wider and shallower eclipse depletions.

The eclipse hole is quite clear in the North with a frontal slope at 0920 UT, while a similar front to North North-East starts at 1010 UT. The hole is deepest in the North North-East where the target is located nearest to the eclipse totality path.

Pre-eclipse oscillations viewed in this three azimuths were widely different; with a strong (non-eclipse) two hour quasi-period wave in the North, a train of three waves of about 50 min in North North-East, and with much weaker fluctuations toward 140°E. Around 0830 UT on 201° and 0900 UT on 24°, a clear increase of group path indicates a North-Eastward moving depletion.

2.3. *Ionogram results*

Fig. 3 shows two sets of data recorded at Francourville and Ebre on August 11 and 12, 1999. The Francourville ionosonde was located just under the total solar eclipse path in the ionosphere between 130 and 250 km height on account of the solar zenithal angle (53° at the maximum obscuration time). The solar obscuration maximum for the Ebre ionosonde was 71%.

Francourville results: Comparing measurements recorded on August 11 and 12, both foF1 variations are identical outside the eclipse time interval, following a Chapman law; inside this time interval, foF1 values on August 11 are lower than on August 12. The maximum photochemical foF1 eclipse fall of 37% is reached at 1023 UT when the Sun is totally eclipsed.

In the F1 layer, the start of the recovery phase (when foF1 begins again to increase) is synchronous with the end of the total solar eclipse (1023 UT). However, the start of the F2 layer recovery phase is 20 min after the local maximum occultation (99%). This observation agrees well with previous results (Cohen (1984): 20–50 min; Salah et al. (1986): 20–30 min; Walker et al. (1991): 20–40 min; Kolokolov et al. (1993): 30–45 min; Afraimovich et al. (1998): 10 min).

Ebre results: The maximum foF1 decrease is reached nearly at the maximum obscuration time with 24%. The 19% fall in foF2 values lags by about 15 min behind the maximum obscuration time.

For the two stations, as also for the other stations not shown here, the foF2 drop during the solar eclipse is weak.

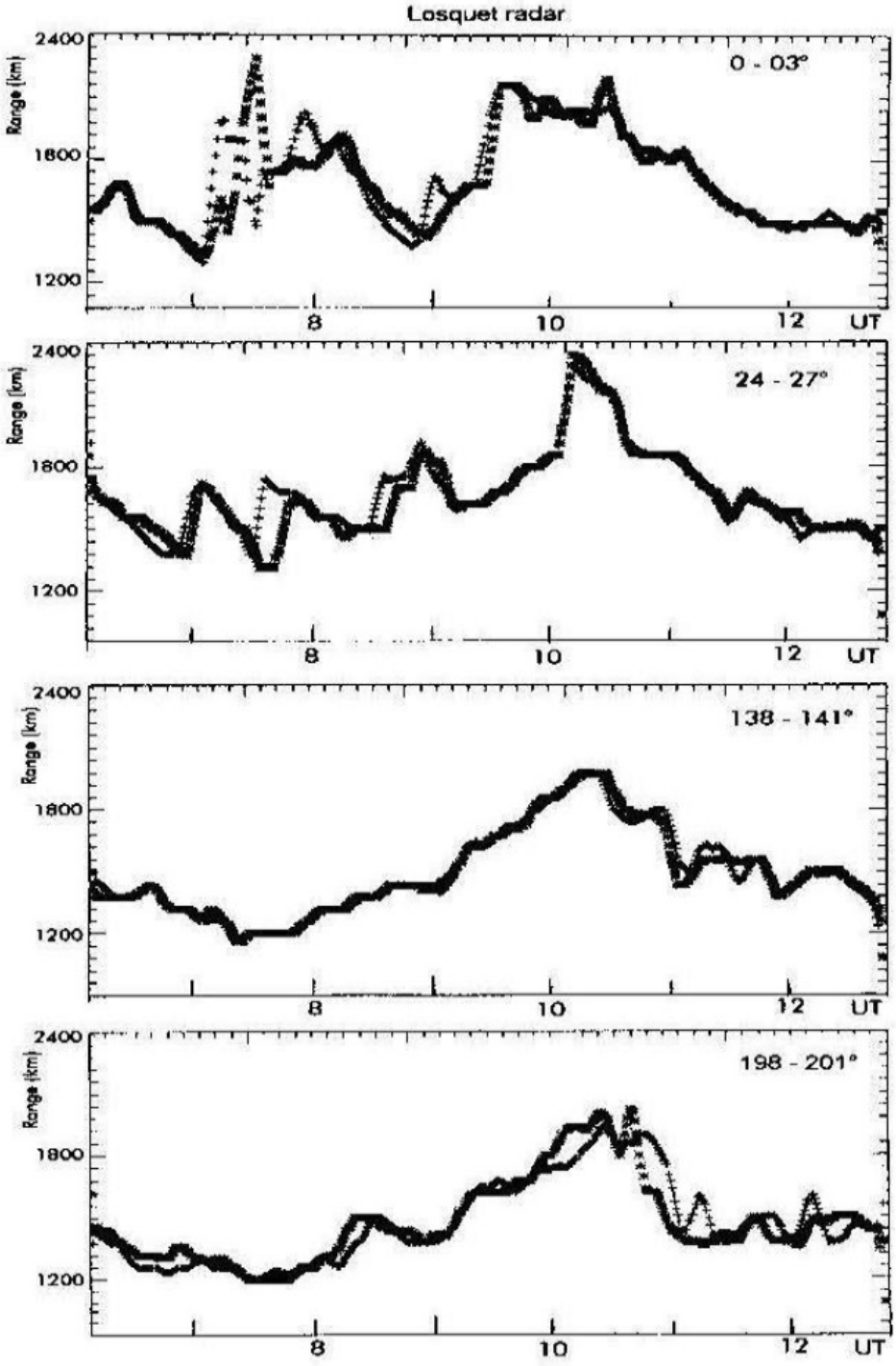

Fig. 2. Return group path versus UT from Losquet Island (Lannion) in four different azimuths: 0–3°, top panel; 24–27°, second panel; 138–141°, third panel and 198–201°, bottom panel.

3. foF1 and foF2 contour maps

Morgan et al. (1978) presented a study with fine space and time resolution showing the evolution of TID. In this paper, we do not use the techniques developed by Morgan et al. For these preliminary results, we present the large time (period of about 2 h) and space (about 1000 km) scale perturbations in the western European ionosphere during the 11 August 1999 solar eclipse with the help of interpolated vertical ionosonde critical frequency maps.

With four ionosondes distributed on the same magnetic meridian, Nagata et al. (1955) had drawn a 2D map of a solar eclipse perturbation at midday in the E region where the x-axis was time and y-axis the distance between ionosondes along the meridian.

Having data from 12 European ionosondes, we build instantaneous maps in 2D extensions for the near-constant heights of hMF1 (about 190 km (Farges, 2000)) and hMF2. Tracing of iso-frequency contours is done using a 2D interpolation method (Akima, 1978).

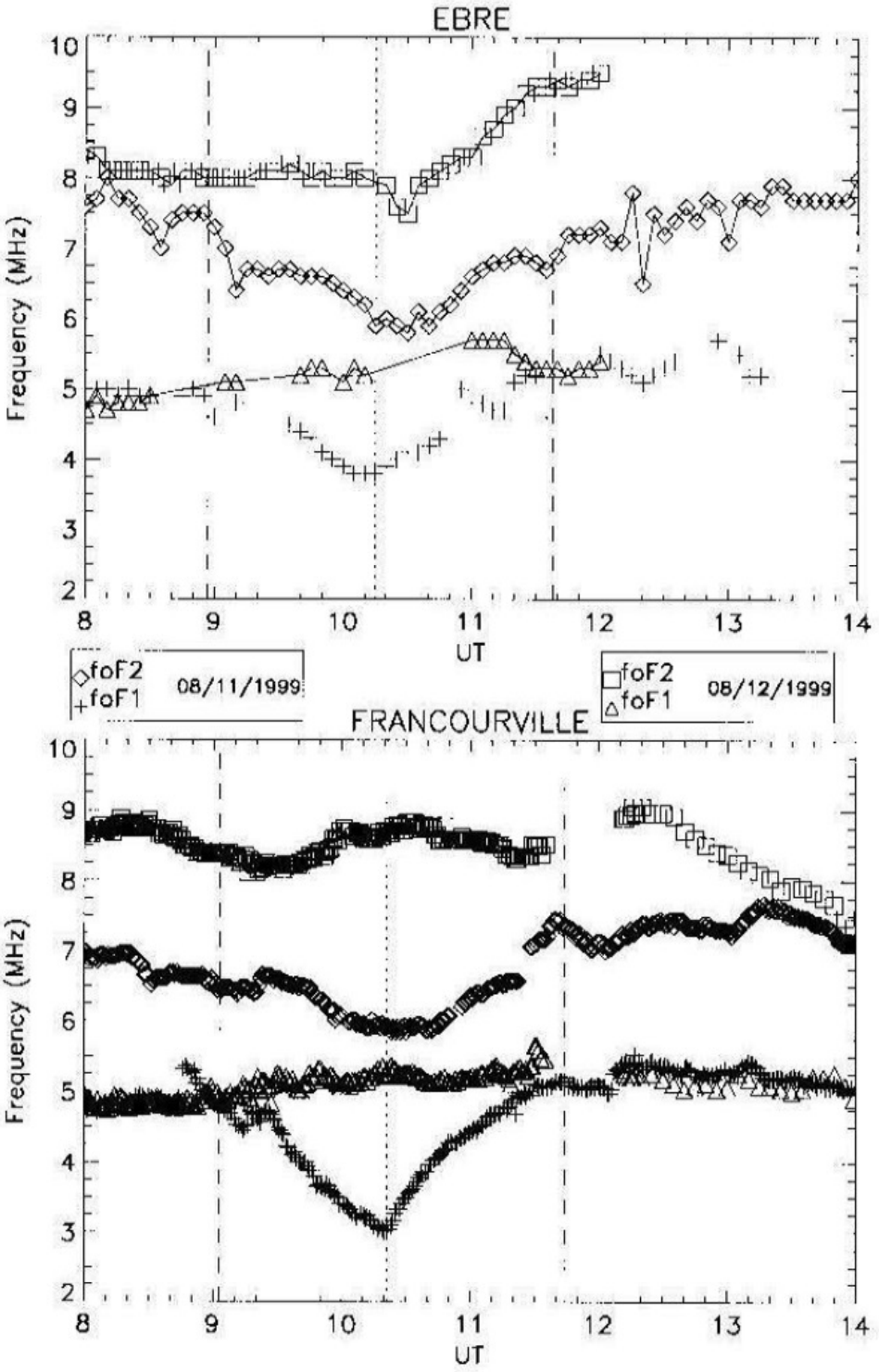

Fig. 3. foF1 and foF2 changes above Francourville and Ebre during the solar eclipse and following hours, the August 11, 1999 and during the same interval of time on August 12, 1999. The start and end times of the solar eclipse are shown with dashed vertical lines; the maximum obscuration time is indicated with a dotted vertical line.

The individual foF1 eclipse time plots are quite accurate (to better than 0.1 MHz except for brief intervals of sporadic E occultation) and clearly minimize at maximum obscuration time. Thus we can use the foF1 parameter space fluctuations as indicators of the eclipse distortions.

Fig. 4 presents ten such quarter-hourly maps between 0830 and 1045 UT and two more at 1200 and 1300 UT. The three sites located further East: Juliusruh, Warshaw and Roma provided data to the tracing as boundary values. A first point deserving notice is the wide latitude extent of the eclipse plasma density depletion, which exceeded 1300 km radius at El Arenosillo (southern Spain).

The eclipse depletion should appear later than 0900 UT from the western longitudes. From 0830 to 0900 UT, the hole observed West of the 0° longitude is probably the last effect of the Atlantic large-scale gravity-wave apparent on the Losquet scans. The eclipse depletion is maximum at 1015 UT. It recedes from 10:45 UT as expected by the

eastward Moon shadow motion. At 1200 UT, the solar eclipse effects disappear completely. This perturbation is too wide (a quasi-circle of diameter much larger than 1000 km) and too fast (around 790 m/s, that is Moon shadow velocity) to be imputed to anything else than the solar eclipse. For instance, the southernmost station El Arenosillo, about 1300 km from totality, measured depletions of −20% on foF1, −17% on foF2.

The peak around Cailhau at 1200 UT is possibly the first sign of an emergent bow wave. At 1300 UT above Ebre, 5.75 MHz contour reveals a frontal peak in F1 layer electron density, that was observed on the individual Ebre plot in

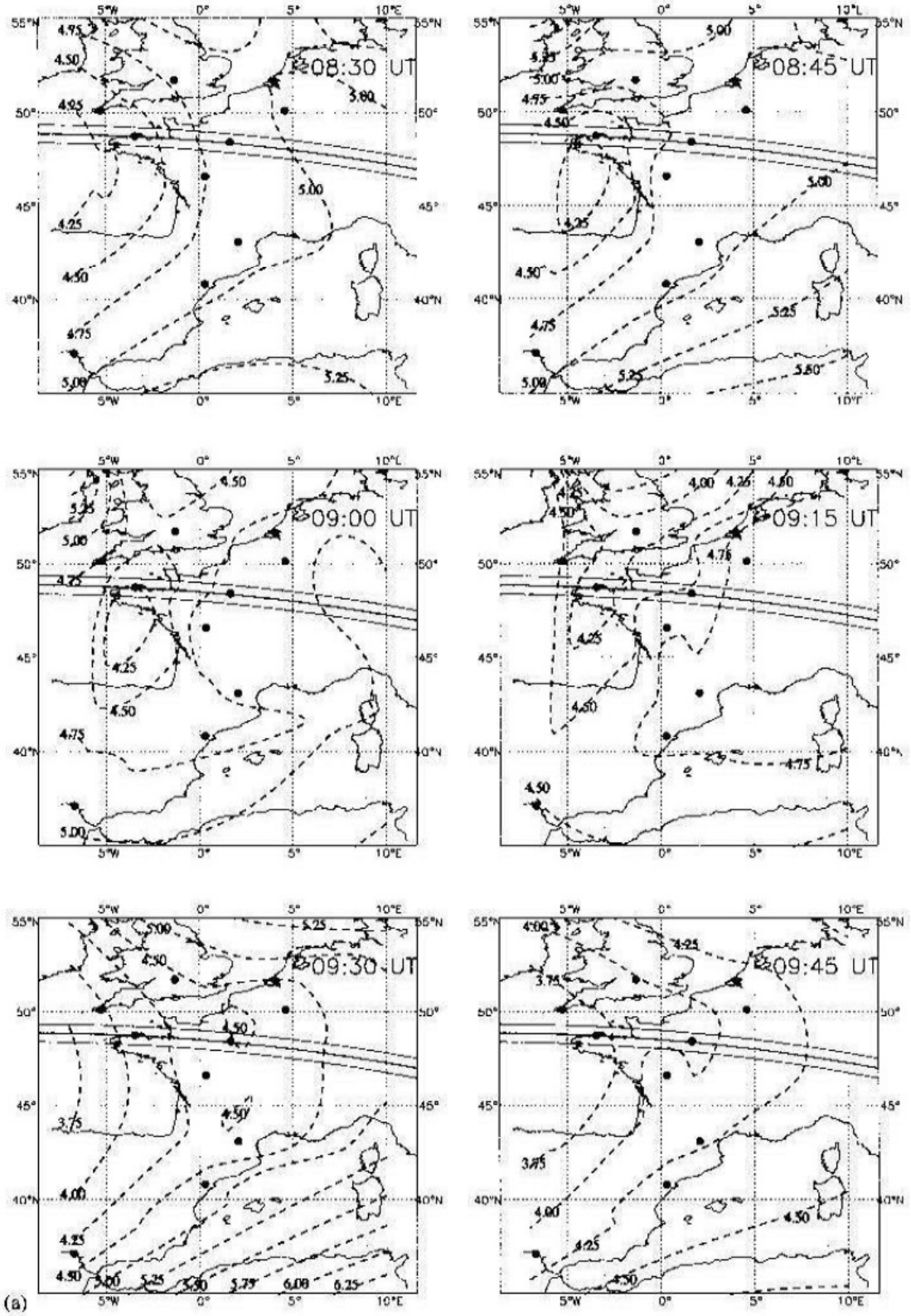

Fig. 4. Contour maps of foF1 quarter-hourly values between 0830 and 1045 UT and between 1200 and 1300 UT drawn on a 50 × 50 km grid. An open circle is drawn on the eclipse path when the Moon shadow is projected on the ionosphere (at 1015 and 1030 UT) at 200 km height above Western Europe.

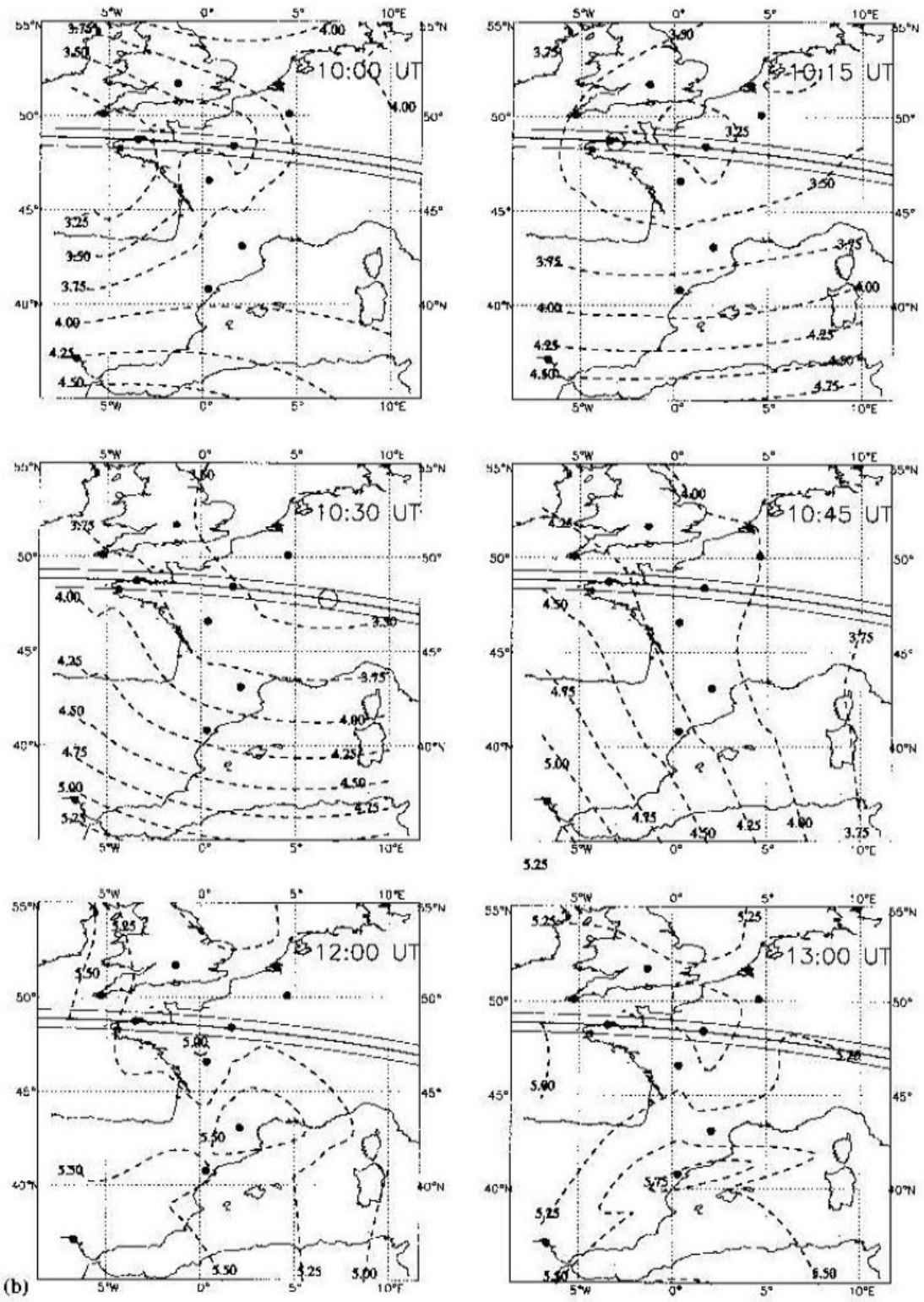

Fig. 4. (*Continued*).

Fig. 3. This wave propagates southward at around 80 m/s. Its properties are discussed in a companion paper (Altadill et al., this issue).

Fig. 5 presents 12 quarter-hourly foF2 maps between 0845 and 1130 UT. The Moon's shadow at 300 km is plotted on the map. The eclipse disturbance is delayed by about 30 min on the maximum obscuration time, as visible in Fig. 3. The 1030 UT map shows a minimum foF2 area centered on 4°W when the Moon's shadow has already reached 7°E.

Two episodes of foF2 depletion occur, respectively, at 0945 and 1100 UT near the 0° longitude and between 45 and 55° latitude.

4. Discussion

The main purpose of our discussion is to relate the two 2D critical frequency maps to the Losquet radar scans.

Consistency between the two sets of measurements would confirm the variations and allow a finer resolution mapping for distances until 1200 km from the Losquet radar.

On Losquet scans, the major phenomenon is observed between 0930 and 1130 UT as a large increase of group path of 300 km. This depletion is obviously due to the eclipse electron density loss.

We will refer to two features most noticeable on the quarter-hourly maps (0845 UT on foF1 and 1100 UT on foF2), and to another effect more apparent on the Losquet scans between 0930 and 1000 UT on the northern azimuths.

(1) We noticed in Section 3 (Fig. 4) the important foF1 hole starting at 0845 in North-West Spain which seems to move to North-East across Brittany toward central England.

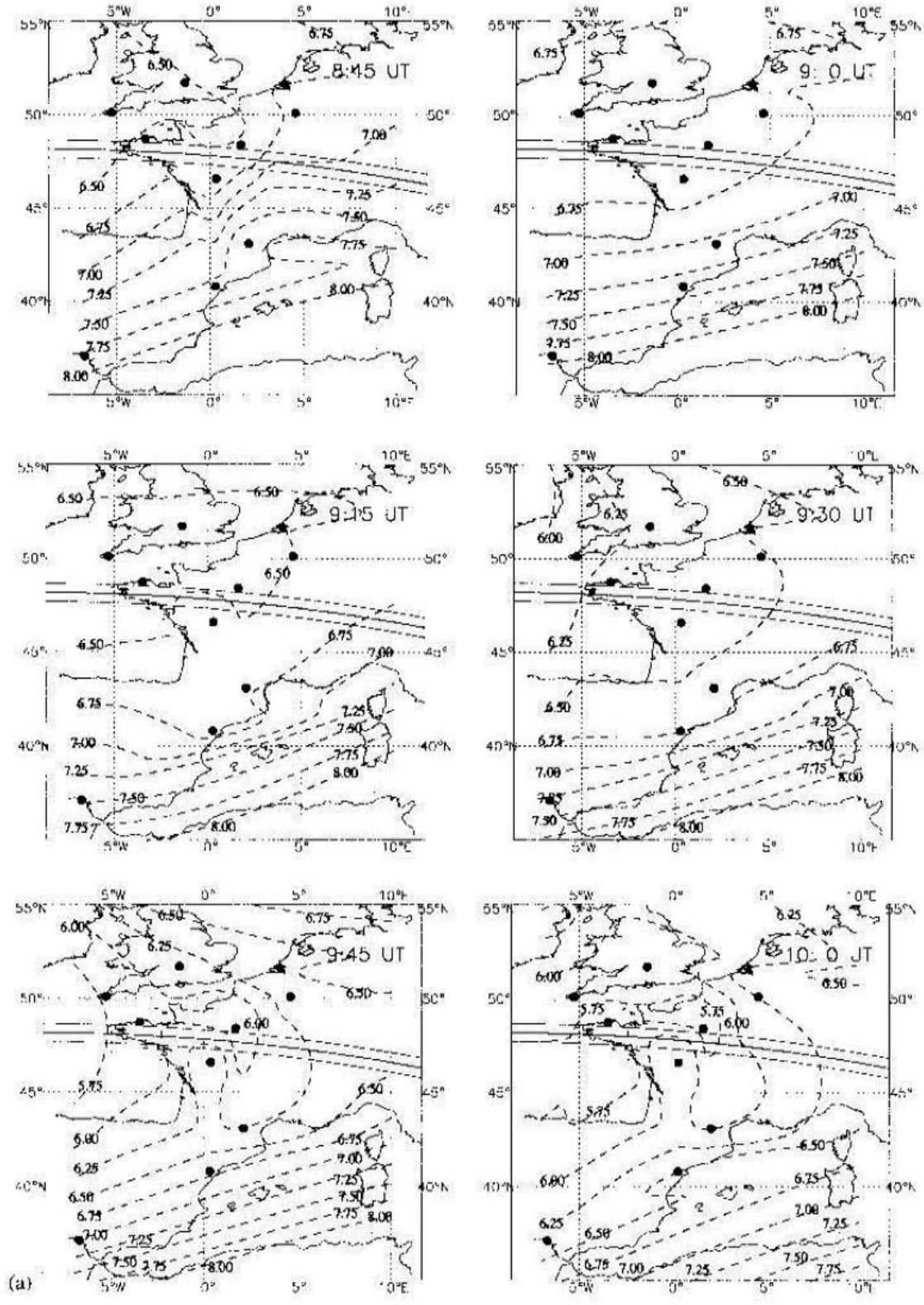

Fig. 5. Contour maps of foF2 quarter-hourly values between 0845 and 1130 UT drawn on a 50 × 50 km grid. An open circle is drawn on the eclipse path when the Moon shadow is projected on the ionosphere (at 1015 and 1030 UT) at 300 km height above Western Europe.

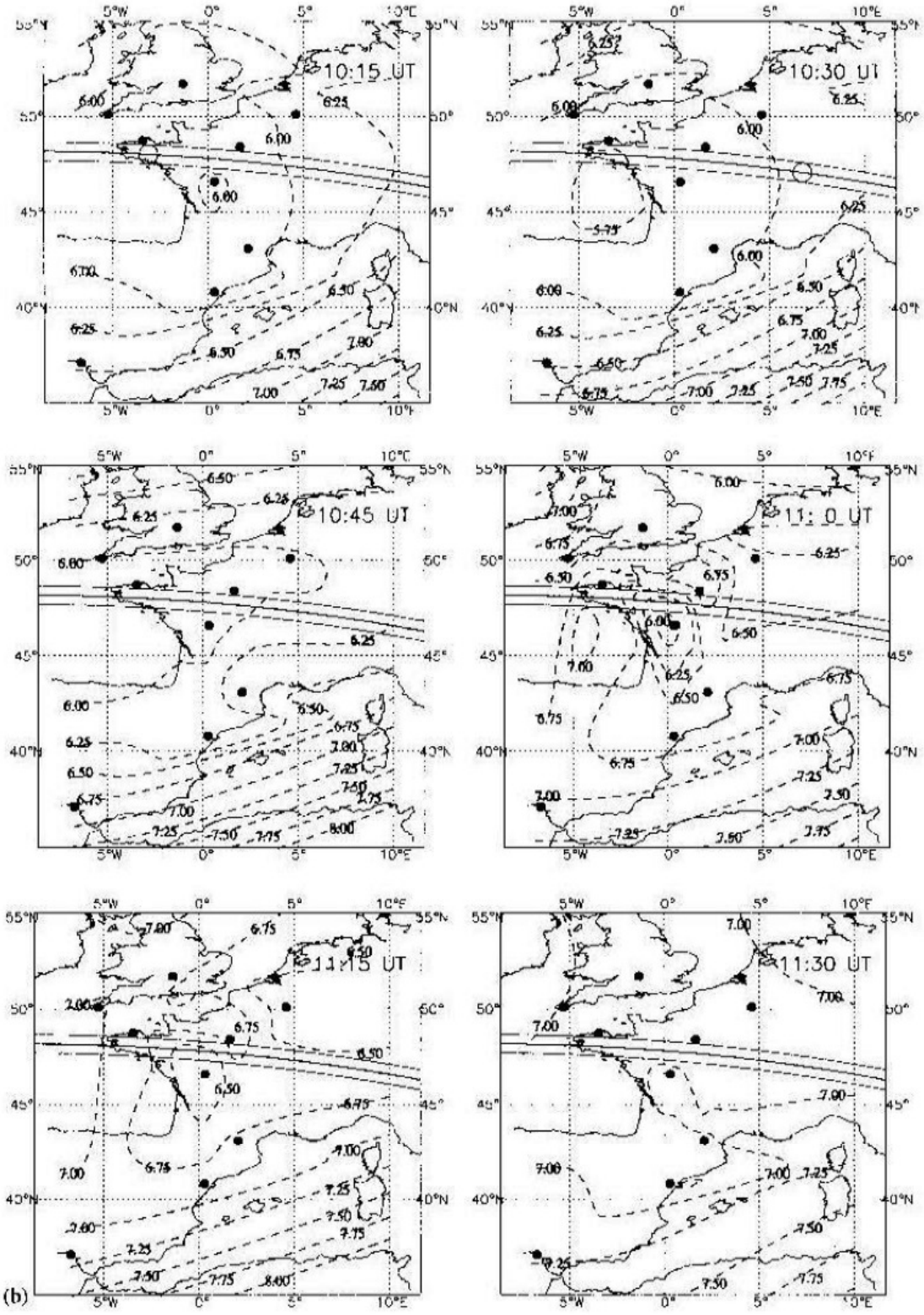

Fig. 5. (*Continued*).

A residual of the foF1 density hole observed on the west area from 0830 to 0930 UT is measured at FRC. The Doppler measurements confirm the North-Eastward displacement. The Losquet scans on 198–201° (0830 UT) and on 24–27° (0900 UT) confirm this depletion and its motion. We cannot presently relate this singularity to any direct eclipse effect. The non-trivial character of this hole and of its displacement is presently difficult to interpret.

(2) The foF2 depletion around Poitiers at 1100 UT (Fig. 5) can be compared with the 138–141° scans from Losquet (Fig. 2). For this area and time, the foF1 variations are uniform; the abnormal reflection is therefore taking place at F2 layer levels between 650 and 900 km group path distance from Losquet. Looking back from Fig. 5 at 1100 UT, we notice a steep density gradient in this direction around the 700 km distance (slightly North of Cailhau). Propagation

on such a steep gradient would justify the abrupt shortening of path distance observed on the Losquet scans (Davies and Rush, 1985).

(3) A third anomaly concerns the time shift of the steep gradient first visible at 0917 from 00° and maintained at 1005 UT on the 24–27° scans. On the northern area the ionosondes are lacking at distances over 250 km from Losquet. Here, the Losquet scans pose a problem that we presently cannot solve with the critical frequency maps. Ray-tracing of our data might be extrapolated sufficiently to North to allow an interpretation of these fluctuations.

5. Summary

The solar eclipse effect in the ionosonde measurements and in the foF1 and foF2 maps is clearly shown as the major effect in the ionosphere. Other main results of this study can be given as follows:

(1) The vertical incidence ionosondes network used for the eclipse campaign allowed us to partly understand the Losquet fine scale variations.
(2) The 20 min time shift of the foF2 minimum relative to the maximum obscuration time at the F2 peak altitude is accurately confirmed for Francourville. At Ebre, the delay is about 25 min.
(3) Everywhere, the F1 density decrease is everywhere synchronous with the eclipse function.
(4) Paradoxical minima at about 0900 UT for the F1 layer and 1100 UT for the F2 layer deserve physical interpretation that will take more work to ascertain.

About this last result, further analysis of the data (for example using with our ionosonde networks the techniques presented by Morgan et al. (1978) and specific simulations (ray-tracing, etc.) should help to differentiate the various modes of ionospheric oscillations.

Acknowledgements

We are indebted for the rapid communication of data from ionospherists not added in the list of authors: Dr. Singer at Juliusruh (Germany), Dr. Stanislawska at Warsaw (Poland), and Prof. Zolesi at Rome (Italy). At Lannion the multiple technical support of M.J. Henry has ensured a decisive contribution, and for Cailhau, the builder of the Very Light Radarsonde, R. Berranger, deserves a mention.

References

Afraimovich, E.L., Palamartchouck, K.S., Perevalova, N.P., Chernukhov, V.V., Lukhnev, A.V., Zalutsky, V.T., 1998. Ionospheric effects of the solar eclipse of March 9, 1997, as deduced from GPS data. Geophysical Research Letters 25, 465–468.

Akima, H., 1978. A method of bivariate interpolation and smooth surface fitting for irregularly distributed data points. ACM Transactions on Mathematical Software 4, 148–159.

Altadill, D., Gauthier, F., Vila, P., Sole, J.G., Miro, G., Saillant, S., Berranger, R, The 11.08.1999 solar eclipse and the ionosphere: the distant bow-wave. Journal of Atmospheric and Solar-Terrestrial Physics 63, 909–914, this issue.

Chimonas, G., Hines, C.O., 1970. Atmospheric gravity waves induced by a solar eclipse. Journal of Geophysical Research 75, 875.

Cohen, E.A., 1984. The study of the effect of solar eclipses on the ionosphere based on satellite beacon observations. Radio Science 19, 769–777.

Davies, K., Rush, C.M., 1985. Reflection of high-frequency radio waves in inhomogeneous ionospheric layers. Radio Science 20, 303.

Farges, T., 2000. Analyse et traitement de données de systèmes radar HF: Etudes des perturbations ionosphériques à l'équateur magnétique avec le radar LDG et à moyenne latitude avec le réseau de Francourville. Ph.D. Thesis, Université de Paris XI, Orsay.

Kolokolov, L.E., Legen'ka, A.D., Pulinets, S.A., 1993. Ionospheric effects associated with solar eclipse of March 18, 1988. Geomagnetism and Aeronomy 33, 41–46.

Morgan, M.G., Calderon, C.H., Ballard, K.A., 1978. Techniques for the study of TIDs with multi-station ionosondes. Radio Science 13, 729–741.

Müller-Wodarg, I.C.F., Aylward, A.D., Lockwood, M., 1998. Effects of a mid-latitude solar eclipse on the thermosphere and ionosphere – a modeling study. Geophysics Research Letters 25, 3787–3790.

Nagata, T., Nakata, Y., Rikitake, T., Yokoyama, I., 1955. Effect of the solar eclipse on the lower parts of the ionosphere and the geomagnetic field. Report of Ionosphere Research in Japan 9, 121–135.

Ratcliffe, J.A., 1956. A survey of solar eclipses and ionosphere. Solar eclipses and the ionosphere. Journal of Atmospheric and Terrestrial Physics 6 (Special suppl.) 1–13.

Ridley, E.C., Dickinson, R.E., Roble, R.G., Rees, M.H., 1984. Thermospheric response to the June 11, 1983, solar eclipse. Journal of Geophysical Research 89, 7583–7588.

Rishbeth, H., 1968. Solar eclipses and ionospheric theory. Space Science Reviews 8, 543–554.

Roble, R.G., Emery, B.A., Ridley, E.C., 1986. Ionospheric and thermospheric response over Millstone Hill to the May 30, 1984, annular solar eclipse. Journal of Geophysical Research 91, 1661–1670.

Salah, J.E., Oliver, W.L., Foster, J.C., Holt, J.M., Emery, B.A., Roble, R.G., 1986. Observations of the May 30, 1984, annular solar eclipse at Millstone Hill. Journal of Geophysical Research 91, 1651–1660.

Walker, G.O., Li, T.Y.Y., Wong, Y.W., Kikuchi, T., Huang, Y.N., 1991. Ionospheric and geomagnetic effects of the solar eclipse of 18 March 1988 in East Asia. Journal of Atmospheric and Terrestrial Physics 53, 25–37.